J. Cell. Mol. Med. Vol 14, No 12, 2010 pp. 2827-2839

Transport characteristics of a novel peptide platform for CNS therapeutics

Yanick Bertrand [a], Jean-Christophe Currie [a], Michel Demeule [b], Anthony Régina [b], Christian Ché [b], Abedelnasser Abulrob [c], Dorothy Fatehi [c], Hervé Sartelet [d], Reinhard Gabathuler [b], Jean-Paul Castaigne [b], Danica Stanimirovic [c], Richard Béliveau [a, *]

[a] *Laboratoire de Médecine Moléculaire, Université du Québec à Montréal, Montréal, Canada*
[b] *Angiochem, Inc., Montréal, Canada*
[c] *Cerebrovascular Research Group, Institute for Biological Sciences, National Research Council of Canada, Ottawa, Canada*
[d] *Department of Pathology, Université de Montréal, Montréal, Canada*

Received: June 2, 2009; Accepted: September 28, 2009

Abstract

New and effective therapeutics that cross the blood-brain barrier (BBB) are critically needed for treatment of many brain diseases. We characterize here a novel drug development platform that is broadly applicable for the development of new therapeutics with increased brain penetration. The platform is based on the Angiopep-2 peptide, a sequence derived from ligands that bind to low-density lipoprotein receptor-related protein-1 (LRP-1), a receptor expressed on the BBB. Fluorescent imaging studies of a Cy5.5Angiopep-2 conjugate and immunohistochemical studies of injected Angiopep-2 in mice demonstrated efficient transport across the BBB into brain parenchyma and subsequent co-localization with the neuronal nuclei-selective marker NeuN and the glial marker glial fibrillary acidic protein (GFAP). Uptake of [^{125}I]-Angiopep-2 into brain endothelial cells occurred by a saturable mechanism involving LRP-1. The primary sequence and charge of Angiopep-2 were crucial for its passage across the BBB. Overall, the results demonstrate the significant potential of this platform for the development of novel neurotherapeutics.

Keywords: blood-brain barrier • therapeutics • drug delivery • Angiopeps • low-density lipoprotein receptor-related protein-1 • receptor-mediated transcytosis • brain disease

Introduction

The central nervous system is physiologically separated from other body compartments by the blood-brain barrier (BBB). The BBB, formed by the endothelial cells of brain capillaries, restricts the exchange of many endogenous molecules between the blood and the brain. In terms of drug development, the very tight regulation of brain homeostasis imposed by the BBB prohibits many small and large therapeutic compounds from entering brain tissue [1]. The BBB has presented a significant challenge to the development of new neurotherapeutics [2–5], and various strategies are currently under development to enhance the uptake of therapeutic compounds into brain parenchyma [6].

We identified a family of peptides, named Angiopeps, that cross the BBB *via* receptor-mediated transcytosis after binding to low-density lipoprotein receptor-related protein-1 (LRP-1) [7]. LRP-1 is highly expressed in brain endothelial cells as well as brain tumour cells, neurons and astrocytes; it is also expressed in the lung, ovary, uterus and liver [8–12]. LRP-1, a large receptor of 600 kD, is a member of the low-density lipoprotein-receptor family [13] and was initially characterized as a clearance receptor for chylomicron remnants [14] and α_2-macroglobulin-proteinase complexes [15].

Proteins that contain a Kunitz-type domain, such as aprotinin, amyloid precursor protein, or tissue factor pathway inhibitor, are substrates for LRP-1-mediated transcytosis. This suggested that Kunitz domain-containing peptides might have the potential to be

*Correspondence to: Richard BÉLIVEAU,
Laboratoire de Médecine Moléculaire,
Université du Québec à Montréal,
CP 8888, succursale Centre-Ville,
Montréal H3C 3P8, Canada.
Tel.: 514-987-3000-X6697
Fax: 514-987-0246
E-mail: oncomol@nobel.si.uqam.ca

doi:10.1111/j.1582-4934.2009.00930.x

advantageously employed to create new drugs with increased brain uptake. We have developed a new antineoplastic agent, ANG1005, which consists of three molecules of paclitaxel conjugated to Angiopep-2, a 19-amino-acid sequence derived from the Kunitz domain present on some LRP-1 ligands. The uptake of ANG1005 into brain parenchyma after *in situ* brain perfusion occurred at a much higher rate than unconjugated paclitaxel, and the agent showed antitumour efficacy in *in vitro* and *in vivo* animal models of brain and lung cancer [16]. ANG1005 is currently under investigation in phase I/II clinical trials for the treatment of primary and secondary brain cancers.

Further characterization of the BBB transcytosis mechanisms of this peptide platform (designated the engineered peptide compound [EPiC] platform) is presented here. Specifically, the biodistribution of Angiopep-2 conjugated to the fluorescent probe Cy5.5 was tracked using small-animal optical infrared imaging [17]. Immunohistochemistry studies co-localized Angiopep-2 with astrocytes and neurons after *in situ* brain perfusion or IV bolus injection. The binding, uptake and transport of Angiopep-2 evaluated in immortalized rat brain endothelial cells (RBE4) demonstrated a role for LRP-1 in its active transport. Results from these studies show that the EPiC platform may have significant potential for the development of other new neurotherapeutics.

Materials and methods

Reagents

Peptides (Angiopep-2, -7, -8 and -79) were synthesized by Peptidec (Pierrefonds, QC, Canada) and Synpep (Dublin, CA, USA). Rabbit polyclonal antibody (pAb) against Angiopep-2 was raised by Cedarlane Laboratories (Burlington, ON, Canada) against Angiopep-2 conjugated with keyhole limpet haemocyanin carrier. After four immunizations at 0, 28, 47 and 66 days, serum was collected at 78 days. The rabbit polyclonal antibody raised against Angiopep-2 was further purified on protein G-Sepharose (Pierce Biotechnology, Rockford, IL, USA), followed by an Angiopep-2-Sepharose affinity column on an ÄKTAexplorer System (GE Healthcare, Baie d'Urfé, QC, Canada). Anti-rabbit IgG horseradish peroxidase-linked secondary antibodies were purchased from Jackson ImmunoResearch (West Grove, PA, USA), and enhanced chemiluminescence reagents were from Amersham Biosciences (Baie d'Urfe, Canada). 4′,6-diamidino-2-phenylindole (DAPI) was from Molecular Probes (Burlington, ON, Canada). Activated α2-Macroglobulin (α2M*) was provided by Dr SV Pizzo (Duke University Medical Center). NHS-Cy5.5 was from GE Healthcare (Baie d'Urfé). The iodo-beads kit and D-Salt Dextran desalting columns were from Pierce Biotechnology. SYBR Green was from Stratagene (La Jolla, CA, USA). Immunomount was from Vector Laboratories (Burlingame, CA, USA). Ultra V block was from Lab vision (Fremont, CA, USA). NeuN was from Molecular Probes. [^{125}I]-Na was from Amersham. Immortalized RBE4 were a gift from Françoise Roux (INSERM, Paris, France). Biotin-streptavidin reagents (LSAB + System HRP Kit) and Diaminobenzidine (DAB) were from Dako (Mississauga, ON, Canada). HiPerFect was from Qiagen (Mississauga, ON, Canada). High capacity cDNA reverse transcription kit was from Applied Biosystem (Faster City, CA, USA). 18S rRNA was from BioCorp (Montreal, QC, Canada). Other biochemical reagents were purchased from Sigma-Aldrich (Oakville, ON, Canada).

Peptide labelling with Cy5.5

Angiopep-2 and Angiopep-7 were labelled with Cy5.5 dye. Briefly, peptides and NHS-Cy5.5 were solubilized in dimethylsulfoxide for the conjugation with the fluorescent probe. Peptide and NHS-Cy5.5 (1.2:1) were incubated with excess triethylamine in the dark for 4 hrs at room temperature by inversion and, then, at 4°C overnight. The coupling was terminated with 4 M hydroxylamine for 30 min. by inversion. The conjugate was then dialysed against phosphate buffered saline (PBS) to remove the dimethylsulfoxyde (DMSO). The labelled peptides were stored at –20°C.

Non-invasive time-domain fluorescence imaging

Methods and protocols used for non-invasive time-domain optical imaging of animals in an EXplore Optix imager (GE Healthcare, Toronto, ON, Canada) were described previously in detail [17, 18]. Briefly, mice received IV injections of 100 μg Cy5.5Angiopep-2 or Cy5.5Angiopep-7 *via* the tail vein. Mice were rapidly anesthetized by inhalation of 4% isoflurane and placed in the imaging compartment. During fluorescent image acquisition, anaesthesia was maintained by mask inhalation of anaesthetic gas mixture with isoflurane. Imaging was performed over periods ranging from 30 min. to 24 hrs. Image analyses and quantifications were performed as described [17, 18] using custom software from Advanced Research Technologies (Montreal, QC, Canada).

Peptide detection by fluorescent microscopy

Fluorescent peptides were injected intravenously *via* the tail vein. Brains were removed, washed, fixed with 3.7% formaldehyde/PBS, permeabilized with 0.1% Triton X-100/PBS, and stained with DAPI for nuclei, tomato lectin for endothelial cells, GFAP antibody for astrocytes and NeuN antibody for neurons as the manufacturer's instructions. Brains were sliced with a vibrotome. Stained tissues were mounted with Immunomount and stored in the dark at 4°C. Fluorescent microscopy images were acquired with a Zeiss LSM510 Meta confocal microscope (Carl Zeiss MicroImaging, Inc., Thornwood, NY, USA).

Histological analysis and immunohistochemistry

Brains were fixed in 10% formalin phosphate and embedded in paraffin. Immunohistochemistry was performed on paraffin-embedded sections using a biotin-streptavidin peroxidase kit in conjunction with an automated Dako immunostainer (Dako). For antigen retrieval, deparaffinized and rehydrated sections were incubated in citrate buffer for 30 min. The sections were then mounted in the Dako autostainer and covered with H_2O_2 for 5 min., followed by a 5 min. application of Ultra V block. The slides were then incubated at room temperature with anti-Angiopep-2 or non-specific mouse or rabbit IgG as negative controls, followed by the addition of the labelled biotin-streptavidin reagents, according to the manufacturer's instructions. DAB was used as a chromogen.

Iodination of angiopep peptides

Peptides were radiolabelled with standard procedures using an iodo-beads kit. A ratio of two iodo-beads per iodination was used for the labelling. Briefly, beads were washed twice with 1 ml of PBS on a Whatman filter and resuspended in 60 μl of PBS, pH 6.5. [^{125}I]-Na (1 mCi) was added to the bead suspension for 5 min. at room temperature. Iodination of peptides was initiated by the addition of 250 μg of protein (100–150 μl) diluted in 0.1 M PBS, pH 6.5. After incubation for 10 min. at room temperature, iodo-beads were removed and the supernatants were applied to a Source^{Tm}15RPC resin (GE Healthcare, Piscataway, NJ, USA) to remove free iodine.

RBE4 cell lines

RBE4 were grown as previously described [1]. Briefly, cells were plated on collagen I-coated plates and maintained in α-minimal essential medium/Ham's F-12 (1:1 [v/v]) medium supplemented with 10% heat-inactivated foetal calf serum, 2 mM glutamine, 300 μg/ml geneticin (G418) and 1 ng/ml basic fibroblast growth factor in humidified 5% CO_2/95% air at 37°C.

[^{125}I]-Angiopep-2 uptake and binding assay

The radiolabelled peptide Angiopep-2 has been shown to be a useful tool for penetrating the BBB [8]. For uptake of [^{125}I]-Angiopep-2, RBE4 cells were seeded at 5×10^4 cells/well in a 24-well plate in appropriate serum media and fed for 3 days. Testing was performed in Ringer/HEPES [137 mmol/l NaCl, 5.36 mmol/l KCl, 0.4 mmol/l Na2HPO4, 0.8 mmol/l $MgCl_2$, 1.8 mmol/l $CaCl_2$, 20 mmol/l N-2-hydroxyethylpiperazine-N′-2-ethanesulfonic acid (HEPES)] adjusted to pH 7.4 with NaOH. Subconfluent cells were incubated with [^{125}I]-Angiopep-2 (final concentration, 100 nM) in the presence or absence of cold Angiopep-2 (quadruplicate determinations) for various times at 37°C. Uptake was done for a 2-min. period, whereas binding was performed for 15 min. at 4°C. Cells were lysed in 0.3 M NaOH and shaken with a Titer Plate Shaker (LAb-Line instruments Inc., Melrose Park, IL, USA) for 30 min. at room temperature. Competitive inhibition of [^{125}I]-Angiopep-2 uptake was performed with poly-l-lysine (350 μg/ml) or protamine (40 μg/ml). Results were quantified with a Wizard 1470 Gamma counter (Perkin Elmer, Woodbridge, ON, Canada). Background radiation of unlabelled cells was subtracted from [^{125}I]-Angiopep-2 values (quadruplicate determinations).

LRP1 silencing and quantitative real-time polymerase chain reaction

RBE4 cells were treated with 100 nM of LRP-1 siRNA or alls stars negative control siRNA for 48 hrs in the presence of the transfecting agent HiPerFect. Total RNA was extracted using Trizol reagent. A cDNA library for each sample was generated with the high capacity cDNA reverse transcription kit according to the manufacturer's protocol. Real-time PCR was performed on an IQ5 multicolour Real-Time Detection System (BIO-RAD, Mississauga, ON, Canada) with PCR Master Mix (SYBR Green). Each reaction contained 20 μl of 2× Master Mix, 1 μM rat LRP-1 forward and reverse primers (Qiagen). One mg of cDNA was used for LRP-1 gene expression. Cycle threshold (Ct) values were normalized to the housekeeper 18S rRNA and comparative quantification was performed based on a 2-Ct calculation method.

In situ mouse brain perfusion

The uptake of [^{125}I]-peptides from the luminal side of mouse brain capillaries was measured using the *in situ* brain perfusion method adapted in our laboratory for the study of drug uptake in the mouse brain [19, 20]. Briefly, the right common carotid artery of ketamine/xylazine-anesthetized mice (140/8 mg/kg, IP) was exposed and ligated at the level of the bifurcation of the common carotid, rostral to the occipital artery. The common carotid was then catheterized rostrally with polyethylene tubing filled with heparin (25 U/ml) and mounted on a 26-gauge needle. The syringe containing the perfusion fluid ([^{125}I]-peptides in Krebs/bicarbonate buffer, pH 7.4, gassed with 95% O_2 and 5% CO_2) was placed in an Harvard PHD 2000 infusion pump (Harvard Apparatus, Holliston, MA, USA) and connected to the catheter. Prior to the perfusion, the contralateral blood flow contribution was eliminated by severing the heart ventricles. The brain was perfused for 5 min. at a flow rate of 1.15 ml/min. After perfusion of radiolabelled molecules, the brain was further perfused for 60 sec. with Krebs buffer to wash away excess [^{125}I]-proteins. Mice were then decapitated to terminate perfusion, and the right hemisphere was isolated on ice before being subjected to capillary depletion. Aliquots of homogenates, supernatants, pellets and perfusates were taken to measure their contents of [^{125}I]-peptides to evaluate the apparent volume of distribution. For capillary depletion, the mouse brain was homogenized on ice in Ringer-HEPES buffer with 0.1% BSA in a glass homogenizer. Brain homogenate was then mixed thoroughly with 35% dextran 70 (50/50) and centrifuged at 5400 × *g* for 10 min. at 4°C. The supernatant composed of brain parenchyma and the pellet representing capillaries were then carefully separated.

Statistical analysis

The data shown are a summary of the results from at least three experiments and are presented as the means ± S.D. Statistical evaluation of the results was performed with Prism software 4.0a. One-way ANOVA by the Kruskal–Wallis method was used when testing three or more groups. The non-parametric Mann–Whitney–Wilcoxon method was used when two groups were compared. Results were considered significant at a value of $P < 0.05$.

Results

Tracking Angiopep-2 with far red fluorescence imaging in brain

We previously reported on the design and synthesis of a family of peptides, called Angiopeps, that were homologous to Kunitz domains identified in human and bovine proteins known to undergo LRP-1 receptor-mediated transcytosis through the BBB [7]. Among them was one designated Angiopep-2, a 19-amino-acid peptide (TFFYGGSRGKRNNFKTEEY) that exhibited high BBB transcytosis *in vitro*. Another peptide, Angiopep-7, was identical to Angiopep-2 except that the lysine residues at positions 10 and 15 were substituted

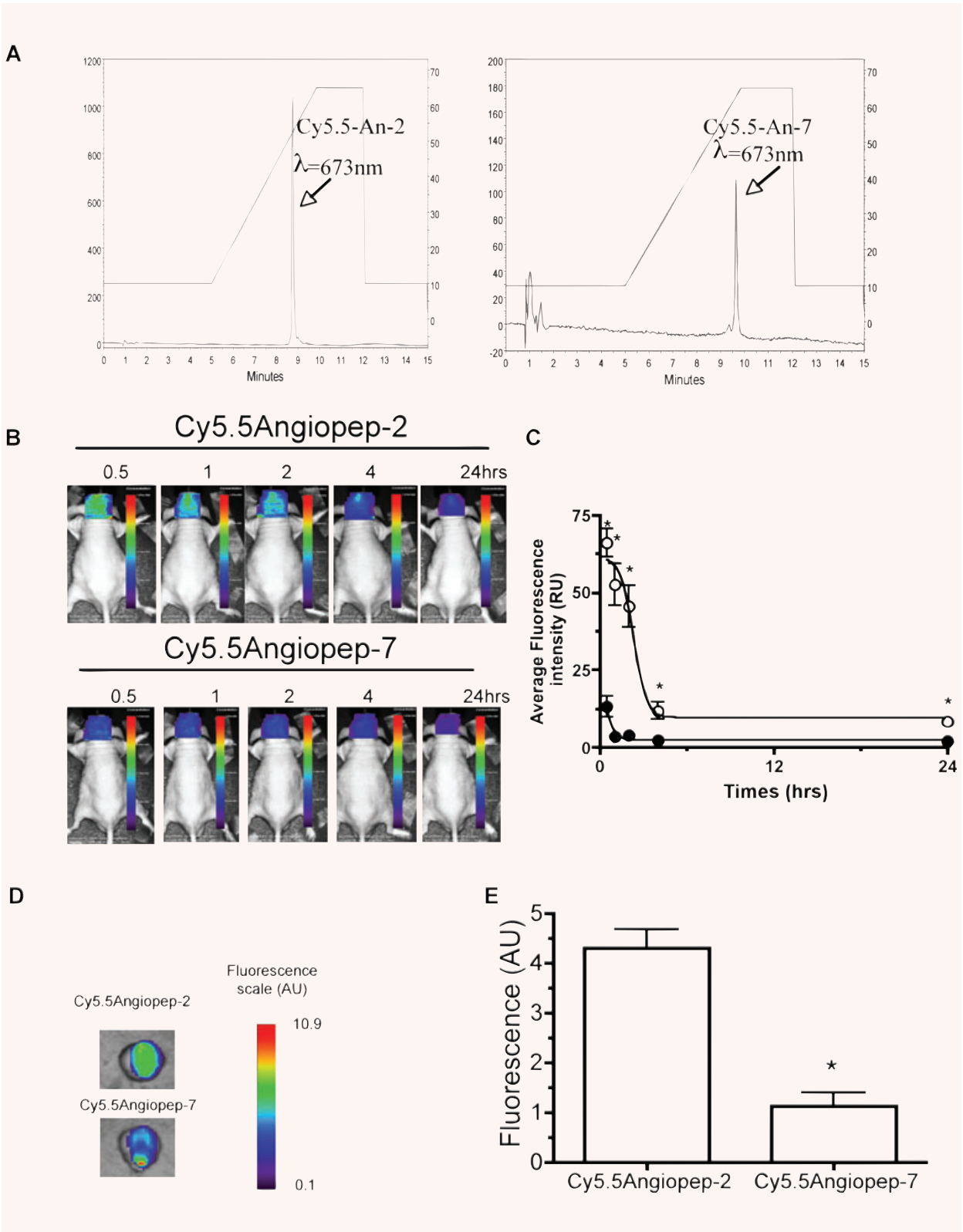

Fig. 1 *In vivo* brain imaging in mice. (**A**) After labelling, both Cy5.5Angiopep-2 (left panel) and Cy5.5Angiopep-7 (right panel) were analysed by HPLC at 673 nm using a Methaxsil (C-18) column and an acetonitrile gradient which is indicated on right *y*-axis (**B**) *In vivo* brain imaging of Cy5.5Angiopep-2 and Cy5.5Angiopep-7 was performed 0.5 to 24 hrs after injection as described ('Materials and methods'). One representative experiment is shown (**C**) Fluorescence intensities in (**B**) was quantified for Cy5.5Angiopep-2 (o) and Cy5.5Angiopep-7 (●) and expressed as a function of time. Error bars, ± S.E.M. (**D**) *Ex vivo* imaging was performed 30 min. after injection of Cy5.5-labelled Angiopeps and whole body perfusion with cold-saline (**E**) Corresponding brain fluorescence intensities are shown in arbitrary units.

with arginine residues (TFFYGGSRGRRNNFRTEEY). Angiopep-7 did not exhibit *in vitro* transcytosis and was used as a negative control in further experiments.

Angiopep-2 and Angiopep-7 were each covalently linked to the near-infrared fluorescent probe Cy5.5 (1 kD), which on its own does not cross the BBB [18]. The two fluorescent conjugates were analysed by HPLC, and the resulting profiles demonstrated single peaks for Cy5.5Angiopep-2 (Fig. 1A, left panel) and Cy5.5Angiopep-7 (Fig. 1A, right panel). HPLC-purified fluorescent molecules were then administered intravenously into the tail veins of mice (100 μg/animal), and brain images were collected at times ranging from 30 min. to 24 hrs after injection using small-animal time-domain optical imaging (Fig. 1B). From these images, brain fluorescence intensities were calculated, and the areas under the curves (AUCs) were extrapolated. The AUC value of Cy5.5Angiopep-2 was 9.5-fold higher than Cy5.5Angiopep-7, demonstrating targeted uptake of Angiopep-2 into brain tissue (Fig. 1C).

To differentiate between the parenchyma and the vascular compartment, *ex vivo* brain images were recorded 30 min. after a bolus injection of either Cy5.5Angiopep-2 or Cy5.5Angiopep-7 followed by a rigorous perfusion with cold saline to remove blood (Fig. 1D). These images indicated a 4-fold higher brain penetration of Cy5.5Angiopep-2 than Cy5.5Angiopep-7 (Fig. 1E). The fluorescence lifetimes (t) of Cy5.5 and Cy5.5Angiopep-2 conjugate were sufficiently different (1.1 and 1.5 nsec., respectively) to be able to differentiate between free dye and dye-peptide conjugate. Analyses of t in organs *ex vivo* 24 hrs after Cy5.5Angiopep-2 injection indicated that the measured t in the brain originated from Cy5.5Angiopep-2 conjugate (data not shown).

Fluorescence microscopy was performed on brain sections either 24 hrs after Cy5.5-labelled peptide bolus IV injection (100 μg/animal) or 2–10 min. after *in situ* brain perfusion with 4 μM of labelled peptide to analyse dye co-localization with specific cellular markers. Brains were then perfused with Krebs solution to wash out dye-labelled peptide from blood vessels and, subsequently, fixed. After bolus IV injection, red Cy5.5Angiopep-2 fluorescence was distributed throughout the parenchyma (Fig. 2A, upper panel), whereas Cy5.5Angiopep-7 fluorescence was below detectable levels (Fig. 2A, lower panel).

After a 2-min. *in situ* brain perfusion, fluorescence derived from Cy5.5Angiopep-2 was observed in both brain capillaries and in the brain parenchyma (Fig. 2B, upper panels) and was higher after a 10-min. perfusion. Cy5.5Angiopep-7 fluorescence was detectable only in intravascular spaces, with no fluorescence detected in the brain parenchyma, after either a 2- or 10-min. perfusion (Fig. 2B lower panels).

Immunofluorescence labelling studies on brain sections with glial marker GFAP (Fig. 2C and D) and neuronal nuclei-selective marker NeuN (Fig. 2E and F) were also performed. Results showed that Cy5.5Angiopep-2 fluorescence was found in the brain parenchyma within the immunoreactive region positively stained for both markers (Fig. 2C and E) [21]. In contrast, Cy5.5Angiopep-7 was undetected under the same conditions in the brain regions labelled with GFAP and NeuN (Fig. 2D and E).

Immunohistochemical detection of Angiopep-2 in brain

A polyclonal antibody (pAb) against Angiopep-2 was generated in rabbits to enable immunohistochemical detection of the peptide in tissues. Western blots performed with serial dilutions of Angiopep-2 indicated that the pAb was able to detect approximately 30 ng of the peptide (Fig. 3A). The antibody detected Angiopep-2 in brain homogenate spiked with Angiopep-2 (2 μg) at the expected molecular weight and with no apparent cross-reactivity to other brain proteins (Fig. 3B).

Using this pAb, Angiopep-2 was detected in brain parenchyma of mice after a 10-min. *in situ* brain perfusion at 37°C with peptide (4 μM) followed by a 60 sec. washout with Krebs buffer (Fig. 3C), but not in control animals perfused with Krebs buffer alone (Fig. 3E). To determine whether similar uptake occurred after IV bolus injection, mice were injected into the tail vein with 20 mg/kg Angiopep-2 or saline, and, after a 60 min. uptake period, were perfused with cold saline to remove excess peptide from the blood. Subsequent immunohistochemistry performed on fixed brain sections showed that Angiopep-2 was present in the brain parenchyma (Fig. 3D), but immunoreactivity levels were lower than those observed after *in situ* perfusion.

Transport mechanism of Angiopep-2 into brain endothelial cells

The uptake of [^{125}I]-Angiopep-2 into RBE4 was characterized as a function of time in the presence of 1 or 50 μM unlabelled Angiopep-2. The addition of unlabelled Angiopep-2 inhibited the uptake of [^{125}I]-Angiopep-2 in a dose-dependent manner (Fig. 4A). To estimate the kinetic parameters of Angiopep-2 uptake in brain endothelial cells, the initial uptake measured at 2 min. was plotted

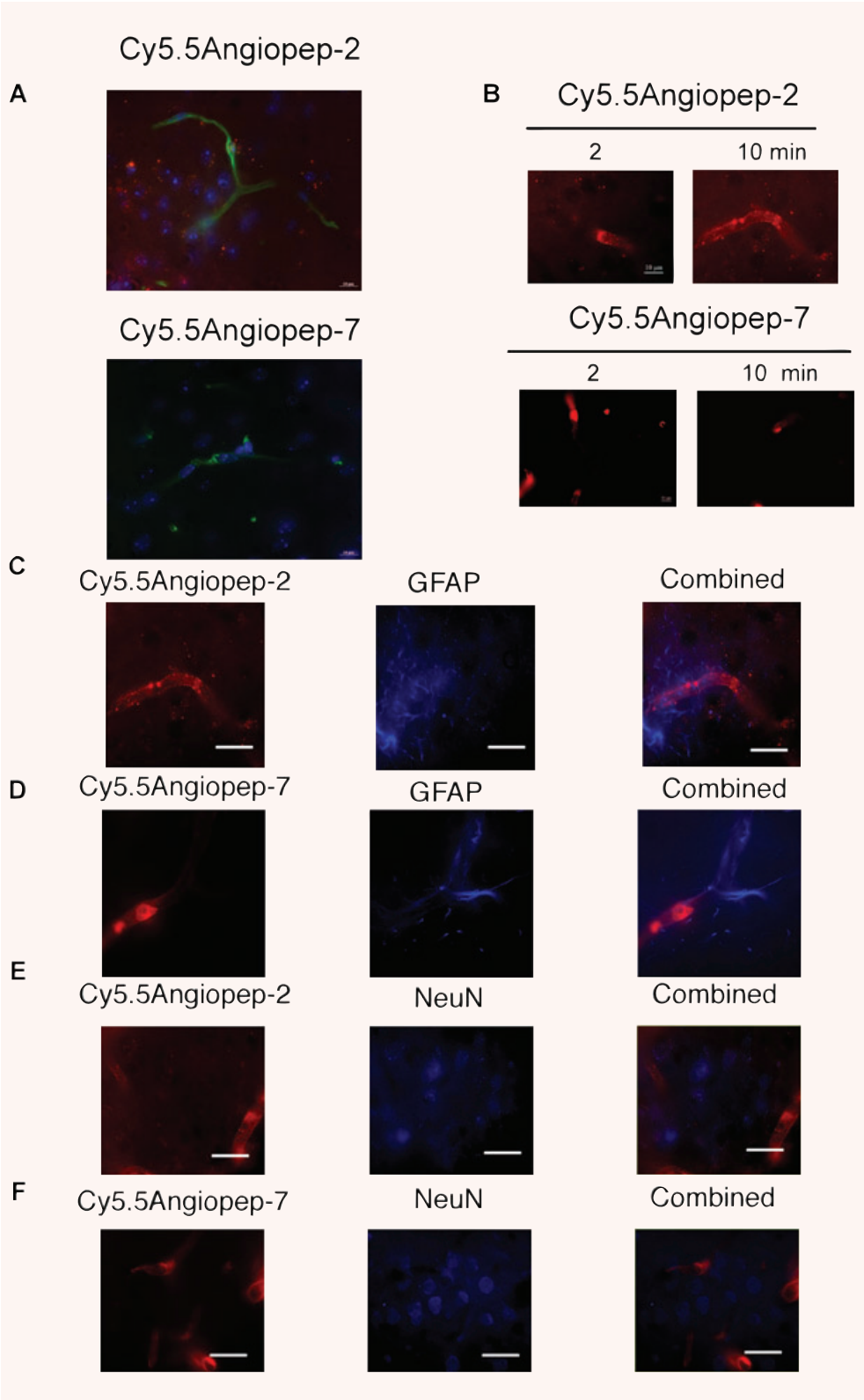

Fig. 2 Fluorescent microscopy of Cy5.5Angiopep-2 and Cy5.5Angiopep-7 in brain sections. (**A**) Twenty-four hours after IV bolus injection of Cy5.5Angiopep-2 or Cy5.5Angiopep-7 (100 μg), brains were fixed and fluorescence microscopy was performed on brain sections. Cy5.5Angiopep-2 was detected as red spots. Nuclei were labelled in blue with DAPI and brain capillaries were labelled in green with tomato lectin. (**B**) Fluorescence microscopy on brain sections after *in situ* brain perfusion for 2 and 10 min. Both Cy5.5Angiopep-2 and Cy5.5Angiopep-7 stain red under these conditions. (**C**) and (**D**) Fluorescent co-detection of the astrocyte (**C**) and neuron (**E**) markers after a 10 min. brain perfusion of Cy5.5Angiopep-2. (**C**) Representative imaging of Cy5.5Angiopep-2 (left panel, in red), astrocyte marker GFAP (middle panel, in blue), and merged images (right panel). (**E**) Representative imaging of Cy5.5Angiopep-2 (left panel, in red), neuron marker NeuN (middle panel, in blue) and merged images (right panel). (**D**) Representative imaging of Cy5.5 Angiopep-7 (left panel, in red), astrocyte marker GFAP (middle panel, in blue) and merged images (right panel). (**F**) Representative imaging of Cy5.5Angiopep-7 (left panel, in red), neuron marker NeuN (middle panel, in blue) and merged images (right panel). The white scale bar represents 10 μm.

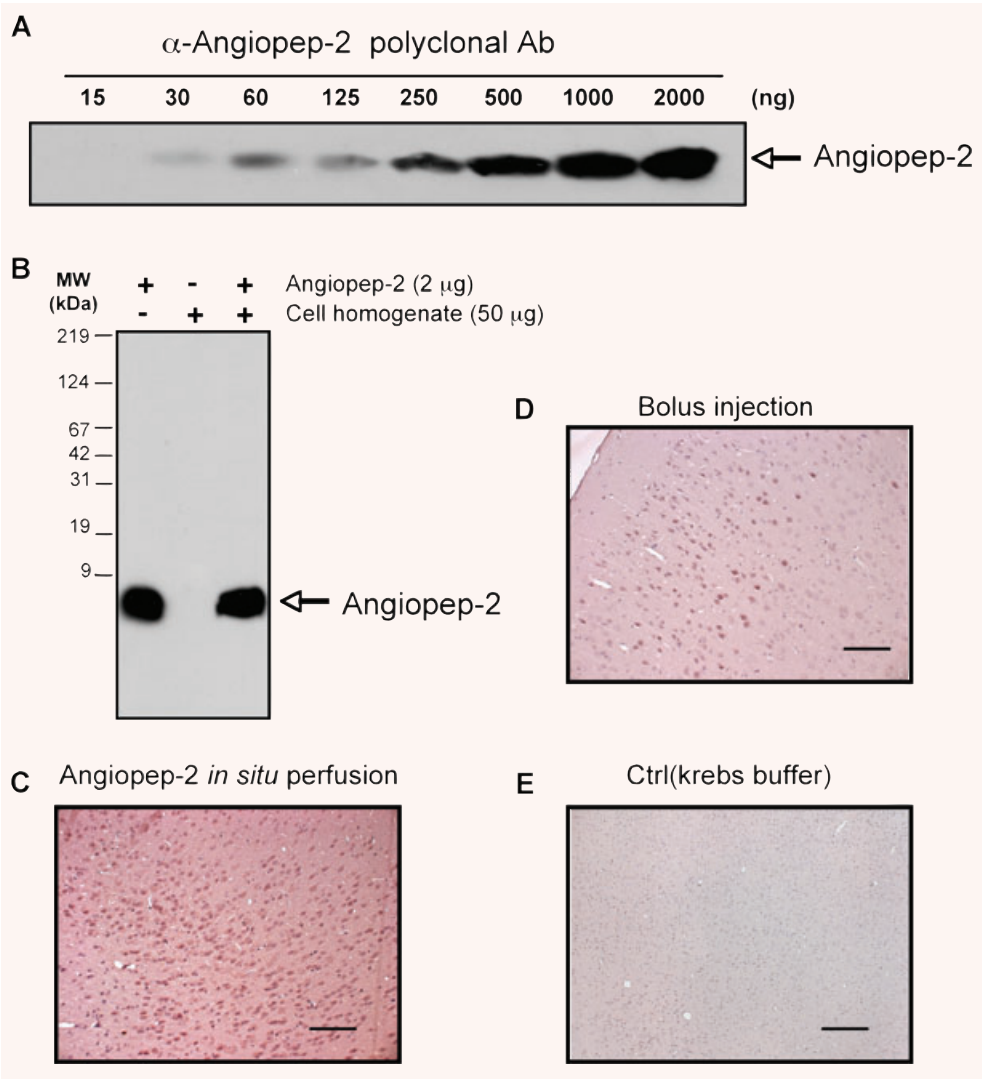

Fig. 3 Immunohistochemistry of Angiopep-2 in mouse brain. (**A** and **B**) Angiopep-2 antibody sensitivity and specificity using Western blot analysis. (**A**) A pAb raised against Angiopep-2 detects various amounts of the peptide (from 30 to 2000 ng) at the expected molecular weight. (**B**) Specificity of the pAb was demonstrated by spiking cell homogenate with Angiopep-2 (2 μg). In cell homogenate, Angiopep-2 is detected at the same migration level. (**C**–**E**) Immunohistochemistry of Angiopep-2 in mice brain. Positive staining is observed after a 10-min. *in situ* brain perfusion with Angiopep-2 (4 μM) (**C**) or 60 min. after IV bolus injection of Angiopep-2 (20 mg/kg) (**D**). Negative control shows absence of staining in brain after Angiopep-2 *in situ* perfusion with Krebs buffer (**E**). The black scale bar represents 50 μm.

as a function of unlabelled concentration of Angiopep-2 (Fig. 4B). The non-specific uptake measured in the presence of the highest concentration of unlabelled Angiopep-2 was subtracted, and results were expressed in terms of Angiopep-2 (pmol/10^6 cells/min.) as a function of total Angiopep-2 concentration (Fig. 4B, insert). The apparent K_m and V_{max} for [^{125}I]-Angiopep-2 were 330 nM and 1.3 pmol/10^6 cells/min., respectively.

We previously reported that LRP-1 ligands inhibited the passage of Angiopep-2 across the BBB in an *in vitro* model system [8]. The role of LRP-1 in Angiopep-2 binding to RBE4 cells was examined here using siRNA designed against rat LRP-1. Under the best silencing conditions, quantitative PCR indicated that LRP-1 mRNA levels (normalized to S18 RNA) were reduced by 40% (Fig. 4C). This reduction correlated with a similar 40% inhibition of [^{125}I]-Angiopep-2 binding to the RBE4 cell surface (Fig. 4D). Under the same silencing conditions, [^{125}I]-α2-macroglobulin binding was inhibited by 50% in siRNA-silenced cells (Fig. 4D).

Effect of charge on Angiopep transport

It has been demonstrated that the polybasic nature of some LRP-1 ligands affects their affinity to the receptor [22]. The influence of charge on Angiopep-2 uptake into RBE4 was assessed using [^{125}I]-Angiopep-2 in the presence or absence of the cationic molecules poly-L-lysine and protamine. Both poly-L-lysine and protamine inhibited Angiopep-2 uptake by 69% and 79%, respectively. In contrast, uptake of Angiopep-2 was unaffected in the presence of the anionic peptide poly-L-glutamine (Fig. 5A). The addition of excess Angiopep-2 with cationic molecules (*e.g.* poly-L-lysine and protamine) did not change uptake of [^{125}I]-Angiopep-2.

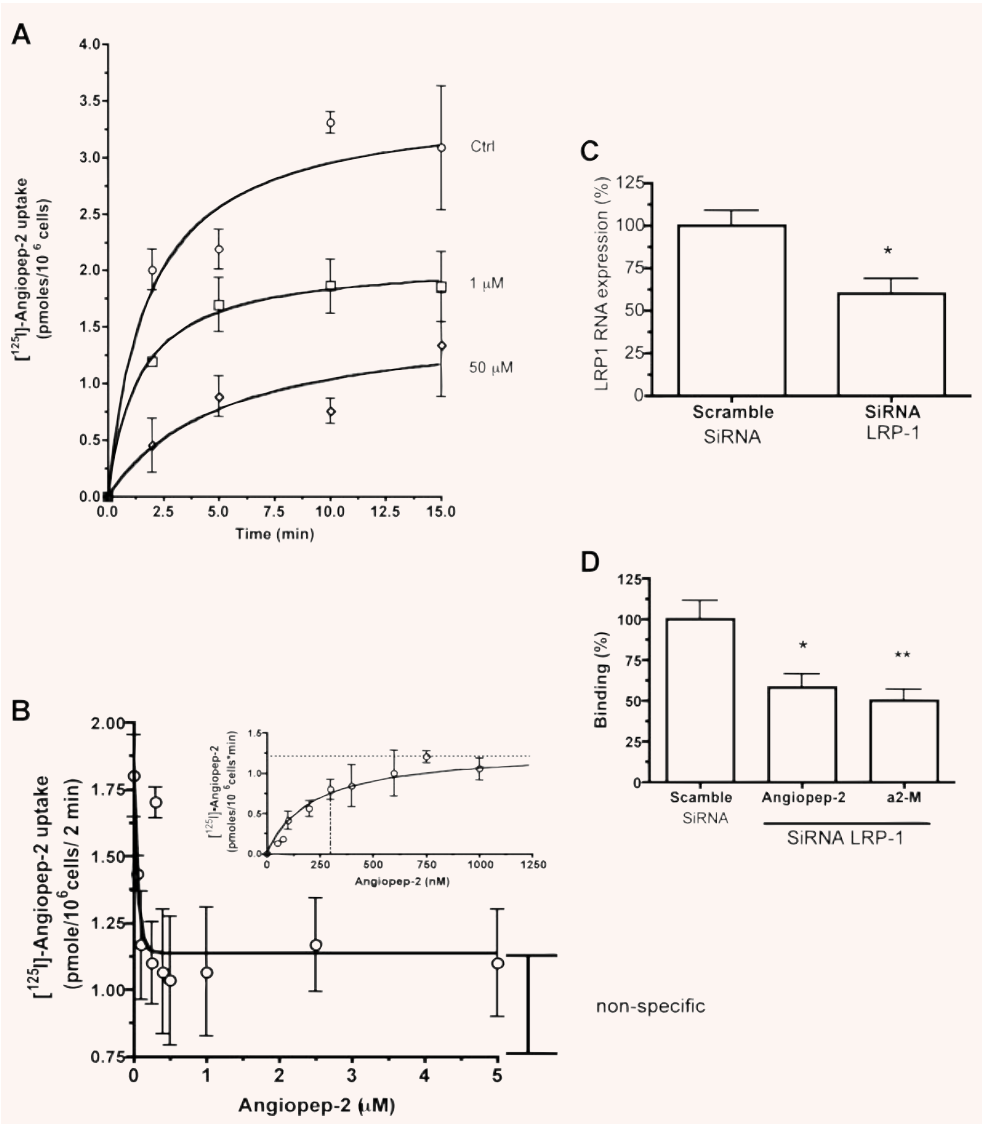

Fig. 4 Determination of Angiopep-2 uptake in brain endothelial cells. (**A**) [^{125}I]-Angiopep-2 uptake was measured for 2, 5, 10 or 15 min. at 37°C in RBE4 cells in the presence or absence of unlabelled Angiopep-2 (1 and 50 μM). (**B**) [^{125}I]-Angiopep-2 uptake in RBE4 was measured at 2 min. in the presence of amid concentrations of Angiopep-2. Non-specific uptake measured in the presence of 50 μM of Angiopep-2 was also subtracted and results expressed in term of pmol/1 × 10^6cells/min. (insert) Data represent the means of three experiments performed in quadruplicate. (**C**) and (**D**) Effect of rat LRP-1 siRNA on LRP-1 gene expression and Angiopep-2 binding in RBE4 cells. (**C**) Down-regulation of LRP-1 gene expression with a specific LRP-1 siRNA in RBE4 cells was measured by real-time qPCR. (**D**) Effect of LRP-1 silencing on [^{125}I]-Angiopep-2 and [^{125}I]-α2-macroglobulin (α2-M) binding, 48 hrs after transfection with LRP-1 siRNA. A scramble siRNA was used as a negative control. Data are expressed as mean ± SD. (*$P < 0.05$ when compared to scramble siRNA)

To further assess the impact of charge on the passage of different Angiopeps into the brain by *in situ* perfusion, the amino acid sequences of these peptides were altered. As described earlier, Angiopep-7 differed from Angiopep-2 in having arginines rather than lysines at positions 10 and 15, but the net charge of these two peptides was constant at +2. Two other peptides, Angiopep-79 and Angiopep-8, had net charges of +4 and +6, respectively (Fig. 5B). *In situ* brain perfusion was performed with iodinated peptides to evaluate their brain volumes of distribution. After capillary depletion, the volume of distribution in total brain, capillaries and parenchyma were higher for Angiopep-2 than for the other peptides. Replacement of the two lysine residues in Angiopep-2 by two arginine residues in Angiopep-7 strongly reduced the BBB transport. The results obtained for two other highly-charged peptides indicated that the total brain volume of distribution increased as a function of the charge. However, this greater volume of distribution was primarily the consequence of a stronger interaction of highly positively-charged peptides with the negatively charged brain vessels, as indicated by the ratio between the volumes of distribution measured for the brain parenchyma (after capillary depletion) and for the total brain (P/B) (Fig. 5B).

Discussion

The data presented here further characterize a new drug-development platform designed to facilitate the isolation of neurotherapeutics with increased brain penetration. The EPiC platform is based on the Angiopep-2 peptide, which is transported across the

A

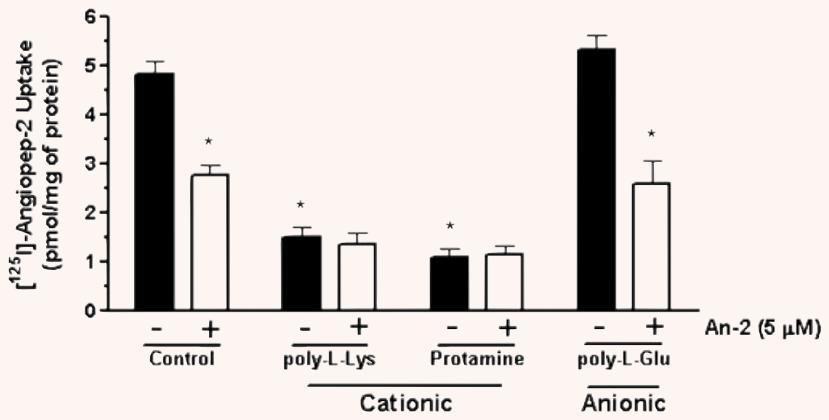

B

Peptides	Charge	*In situ* Brain Perfusion Vd (ml/100g/5min)			
		Brain B	Capillaries C	Parenchyma P	Ratio P/B
Angiopep-2	**+2**	24	4	20	0.84
Angiopep-7	**+2**	5.4	2.4	3	0.55
Angiopep-79	**+4**	70	52	18	0.26
Angiopep-8	**+6**	250	204	46	0.18

Fig. 5. Effects of charge on Angiopep-2 brain transport. (**A**) Uptake of [^{125}I]-Angiopep-2 (100 nM) in RBE4 cells was also measured in the presence or absence of poly-L-lysine (350 μg/ml) or protamine (40 μg/ml) with or without unlabelled Angiopep-2 (5 μM). (**B**) Brain perfusion of [^{125}I]-Angiopep-2 and Angiopep-2 analogues (250 nM) in mice was performed for 5 min. The amino acid sequences, net charge and distribution volume in the brain compartments for these peptides are shown. Data represent the means ± S.D. obtained from at least three different mice for each peptide.

BBB *via* LRP-1 receptor-mediated endocytosis. In initial validation studies, Angiopep-2 was shown to efficiently cross bovine brain capillary endothelial cell monolayers in an *in vitro* transcytosis assay and to have a greater apparent distribution volume in brain parenchyma than transferrin after *in situ* perfusion [23]. Furthermore, *in vivo* injection of ANG1005, a new chemical entity containing Angiopep-2 and the antineoplastic drug paclitaxel, inhibited growth of orthotopic human glioblastoma (U87 MG) brain tumours in mice more potently than paclitaxel alone and significantly increased animal survival rate [16].

A primary objective of the current study was to improve our understanding of the biodistribution and cellular localization patterns of Angiopep-2 and Angiopep-2-derived agents after systemic injection. In previous studies [16, 23], brain distribution of Angiopep-2 was assessed after *in situ* brain perfusion using a physical separation technique [24] that enriched for brain parenchyma by homogenizing whole cerebral lobes and, subsequently, depleting vascular capillaries by differential centrifugation. This approach demonstrated efficient uptake of Angiopep-2 into gross parenchymal tissue, but did not characterize its distribution at the cellular level. In this report, whole animal fluorescence studies, fluorescence microscopy and immunohistochemical studies confirmed that Angiopep-2 and Cy5.5Angiopep-2 crossed the BBB and accumulated in brain parenchyma. The fluorescence pattern of Cy5.5Angiopep-2 after *in situ* brain perfusion and IV injection was diffuse and homogenous throughout brain parenchyma, while at the cellular level the fluorescence co-localized broadly with neurons and astrocytes in brain sections. It should be noted that the fluorescence study showed uptake of Cy5.5Angiopep-2 in both *in situ* brain perfusion and bolus injection.

The observed localization results are consistent with the underlying biology of the system. Thus, the broad distribution pattern likely reflects the fact that capillary density in the cerebrum is extraordinarily high, with virtually every neuron perfused by its own vessel [25]. Additionally, LRP-1, which participates in transporting Angiopep-2 across the BBB, is abundantly expressed on brain capillaries [26, 27]. The immunofluorescence results with GFAP and NeuN suggest that after passing through the BBB, Angiopep-2 could reach neurons and astrocytes. Both of these parenchymal cell types are known to express LRP-1 [28–32]; however, the involvement of this receptor in the internalization of Angiopep-2 remains to be clearly demonstrated. Another formal possibility is that Angiopep-2

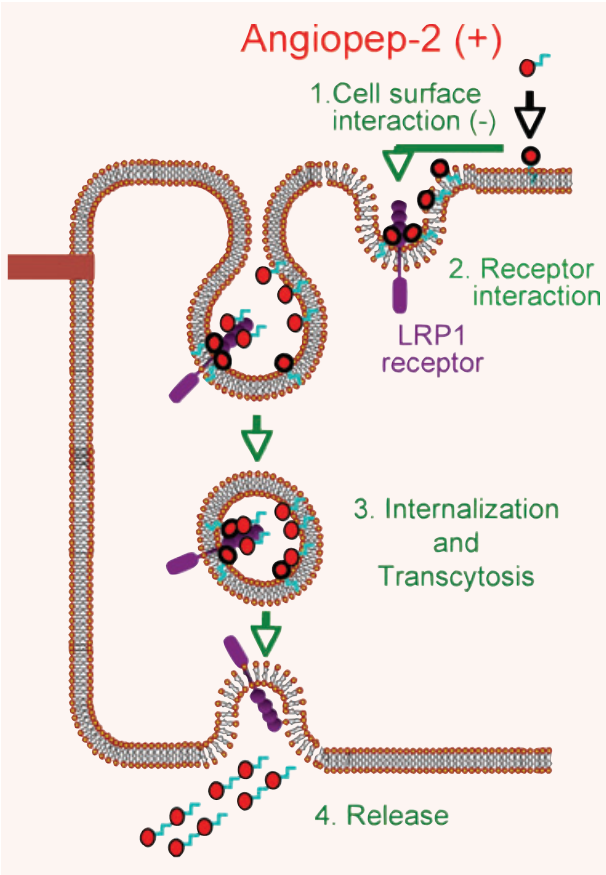

Fig. 6 Schematic representation of Angiopep-2 passage across the BBB. This model summarizes the data obtained for the interaction of Angiopep-2 (in red circle) with endothelial cell surface (1) and for the involvement of LRP-1 (in purple) in the binding (2), transcystosis (3) and release (4) of this peptide.

remains bound to neuronal and astrocytic membranes, without true endocytosis. Previous data indicate that ANG1005 has significant antineoplastic activity in mice following intracerebral implantation of U87 MG glioblastoma cells [23] and enters into tumour tissue in human patients with primary gliomas (Angiochem, Inc., unpublished). Moreover, ANG1005 increases survival of mice after intracerebral implantation of NCI-H460 lung carcinoma cells [23] and exhibits antineoplastic activity in patients with secondary brain metastases of either non-small-cell lung carcinoma or ovarian cancer (Angiochem, Inc., unpublished). Because antineoplastic activity of the paclitaxel moiety depends upon intracellular uptake, and because LRP-1 is expressed on gliomal, lung and ovarian cells [8–12, 33], these data are consistent with true endocytosis of Angiopep-2 agents into parenchymal cells after passage through the BBB, but further confirmatory studies are warranted. It should also be noted that these data may suggest that therapeutics developed by the EPiC platform could be particularly well-suited for other non-brain diseases characterized by expression of LRP-1.

Previous transport data, as well as data on the inhibition of transport with other LRP-1 ligands, suggested that Angiopep-2 penetrated brain tissue *via* LRP-1 receptor-mediated transcytosis [34]. In this study, kinetic parameters for Angiopep-2 transport in RBE4 demonstrated the involvement of a receptor with an apparent affinity of 313 nM, similar to the affinity of tPA to LRP-1 [35]. This affinity was lower than that of receptor-associated protein (RAP) or α2-macroglobulin, which have affinities for LRP-1 of approximately 2 nM in other cell types [36]. Nonetheless, the capacity for Angiopep-2 transport may be greater than these other proteins [37]. The increased passage into brain parenchyma provides Angiopep-2 with a clear advantage over other LRP-1 ligands, such as RAP [38]. In addition, we observed that Angiopep-2 internalization or uptake occurred rapidly. Rapid uptake of Angiopep-2 *via* an LRP-1-mediated mechanism is in agreement with a previous study demonstrating LRP-1 internalization in less than 5 min. for two LRP-1 ligands: Aβ and tPA [39]. A previous study showed that internalization of the fl-amyloid peptide by LRP1 induced death of cerebral perivascular cells *in vitro* [12]. It is important to note that Angiopep-2 has no sequence homology with the fl-amyloid peptide and that endothelial cells exposed to Angiopep-2 were unaffected (data not shown). Furthermore, the permeability of the BBB to inulin was unaffected in the presence of Angiopep-2 during *in situ* brain perfusion [40], indicating that Angiopep-2 does not affect the integrity of the BBB.

Cy5.5Angiopep-2 crossed the BBB following *in situ* brain perfusion, but Cy5.5Angiopep-7 was only detected intravascularly. Moreover, *in vivo* imaging studies demonstrated a 9.5-fold higher brain fluorescence intensity of Cy5.5Angiopep-2 than Cy5.5Angiopep-7. These results demonstrate the importance of the peptide's primary sequence in the transcytosis mechanism (see below). At the amino acid level, the only differences between Angiopep-2 and Angiopep-7 were the replacement of two lysines by arginines in Angiopep-7. The results were consistent with prior published observations showing that the replacement of these two lysines in aprotinin diminished its affinity for LRP-1 and LRP-2 (megalin) [22]. Similarly, RAP, an LRP ligand and known competitor for Angiopep-2 transcytosis across the BBB [8], displayed a drastically reduced affinity for LRP-1 when mutated at lysines 256 and 270 [41].

Another line of evidence supporting a direct involvement of LRP-1 in Angiopep-2 interaction with brain endothelial cells comes from RNA silencing experiments. RNAi knockdown of LRP-1 decreased Angiopep-2 binding. Under the same silencing conditions, the binding of α_2-macroglobulin, the most specific LRP-1 ligand [42], was also inhibited. These LRP-1 silencing results are similar to a recent study in which a 40% decrease in LRP-1 expression by siRNA reduced the binding of two other LRP-1 ligands (tPA and Aβ) to brain endothelial cells [39]. Angiopep-2 uptake into brain endothelial cells was inhibited by polycationic peptides. It has been reported that the cellular entry of peptides depends on their surface charge, which may be crucial in mediating their initial interaction with the cell membrane

[22, 43]. Cationic polyamines like protamine are also known to affect LRP-1 binding to its ligands [44]. The effect of cationic polyamines on [^{125}I]-Angiopep-2 uptake demonstrated the contribution of charge to this process. Previous studies [45, 46] and *in situ* brain perfusion results shown here indicated that the charge of Angiopeps affected their partition between brain compartments and that the primary sequence of Angiopep-2 provided LRP-1 transport specificity. Interestingly, it has been demonstrated that other receptors of the LDL-family are also expressed at the BBB [47]. Because they could share ligands, we cannot exclude the possibility that other members of this family could also be involved in this process. Other receptors at the BBB, such as the organic anion-transporting polypeptides (OATPs) [48] or the receptor for advanced glycation end products, which has been demonstrated to transport fl-amyloid [49], could also be other candidates. Experiments are currently underway to further elucidate the transcytosis and trafficking of Angiopep-2 across the BBB. However, the inhibition of Angiopep-2 uptake in RBE4 cells by LRP1 siRNA and by positively charged peptides suggest that the charges and LRP-1 are responsible for the major mechanism of transport for Angiopep-2 across the BBB.

Data obtained on the transport mechanism of Angiopep-2 are summarized in Fig. 6. The results presented here suggest that the positive charge of Angiopep-2 (+2) contributes to its binding to the brain endothelial cell surface. After its interaction with LRP-1, the Angiopep-2/LRP-1 complex is internalized by vesicle formation. Because of the involvement of LRP-1, Angiopep-2 crosses the BBB in a fashion that can be distinguished from other cell-penetrating peptides (CPPs) such as TAT, penetratin and Syn-B, which use adsorptive-mediated transcytosis [50]. When the charge on Angiopep was increased to CPP levels, the peptides were trapped in the BBB, as demonstrated by Angiopep-79. Scrambled CCPs retained the internalization properties of their parent peptides, indicating that internalization is unrelated to their specific primary sequences [51], but appears to depend instead on negatively charged cell surface components [52]. Again, Angiopep-2 can be distinguished from classic CCPs in that small modifications to the primary sequence greatly affected the level of brain uptake.

A variety of therapeutic approaches to cross the BBB have been examined previously, but most have been unsuccessful and/or inconvenient (reviewed in [5, 53, 54]). For instance, delivery of agents through a physically disrupted BBB, produced by intracarotid infusion of solvents, immune adjuvants, cytokines, or hyperosmolar, vasoactive or alkylating agents, has proven unworkable. Non-specific diffusion of drugs through brain capillary endothelia has been successful for some agents, but has been severely hampered by the constraint that such diffusion is only feasible for very small (<400–500 Da) and highly lipophilic (<8–10 hydrogen bonds) agents. Finally, the transfer of neurotherapeutic agents *via* specific transporter systems, which typically demands that a new pharmaceutical be structurally similar to the endogenous substrate, has been difficult to achieve in practice, although it has been successfully applied in individual cases (*e.g.* L-Dopa for Parkinson's disease).

The EPiC platform provides a number of important advantages over these prior approaches. First, because LRP-1 is distributed widely on brain capillaries, the BBB transfer appears to occur efficiently and broadly throughout brain parenchyma. Second, because it is relatively straightforward to separate receptor binding and pharmacologic action domains within a single therapeutic molecule, structural constraints imposed on drug design are less onerous than those associated with specific transport or non-specific diffusion. Finally, receptor-mediated transcytosis should be compatible with small and large ligands, as well as ligands of different charge or lipophilicity. Overall, neurotherapeutics comprise a relatively small proportion of the available pharmacopeia [55, 56], and it has been argued that one of the main limitations preventing their development has been the BBB [4, 5, 53, 54]. The results presented here and in earlier studies [23, 40] suggest that the EPiC platform may have significant utility in overcoming this constraint on the development of novel neurotherapeutics.

Acknowledgements

We thank Julie Poirier, Isabelle Lavallée, Tran Nguyen and Marie-Claude Lacoste for their technical support. This work was supported by research funding from the National Research Council of Canada's Industrial Research Assistance Program (NRC-IRAP) to Angiochem and from the Natural Sciences and Engineering Research Council of Canada (NSERC) to R.B. The authors also thank David Norris, Ph.D. for editorial assistance provided during the preparation of this manuscript. This assistance was paid for through funding supplied by Angiochem to Ecosse Medical Communications, LLC (Princeton, NJ).

References

1. **Roux F, Couraud PO.** Rat brain endothelial cell lines for the study of blood-brain barrier permeability and transport functions. *Cell Mol Neurobiol*. 2005; 25: 41–58.
2. **Pardridge WM.** Blood-brain barrier drug targeting: the future of brain drug development. *Mol Interv*. 2003; 3: 90–105, 51.
3. **Pardridge WM.** The blood-brain barrier: bottleneck in brain drug development. *NeuroRx*. 2005; 2: 3–14.
4. **Cecchelli R, Berezowski V, Lundquist S, *et al.*** Modelling of the blood-brain barrier in drug discovery and development. *Nat Rev Drug Discov*. 2007; 6: 650–61.
5. **Pardridge WM.** Drug targeting to the brain. *Pharm Res*. 2007; 24: 1733–44.
6. **Dove A.** Breaching the barrier. *Nat Biotechnol*. 2008; 26: 1213–5.
7. **Demeule M, Regina A, Che C, *et al.*** Identification and design of peptides as a new drug delivery system for the brain. *J Pharmacol Exp Ther*. 2008; 324: 1064–72.
8. **Demeule M, Currie JC, Bertrand Y, *et al.*** Involvement of the low-density lipoprotein receptor-related protein in the transcytosis of the brain delivery vector angiopep-2. *J Neurochem*. 2008; 106: 1534–44.
9. **Acarregui MJ, England KM, Richman JT, *et al.*** Characterization of CD34+ cells isolated from human fetal lung. *Am J Physiol*

Lung Cell Mol Physiol. 2003; 284: L395–401.

10. **Mahley RW, Huang Y.** Atherogenic remnant lipoproteins: role for proteoglycans in trapping, transferring, and internalizing. *J Clin Invest*. 2007; 117: 94–8.
11. **Zhang C, An J, Strickland DK, *et al.*** The low-density lipoprotein receptor-related protein 1 mediates tissue-type plasminogen activator-induced microglial activation in the ischemic brain. *Am J Pathol*. 2009; 174: 586–94.
12. **Wilhelmus MM, Otte-Holler I, van Triel JJ, *et al.*** Lipoprotein receptor-related protein-1 mediates amyloid-beta-mediated cell death of cerebrovascular cells. *Am J Pathol*. 2007; 171: 1989–99.
13. **Herz J, Strickland DK.** LRP: a multifunctional scavenger and signaling receptor. *J Clin Invest*. 2001; 108: 779–84.
14. **Beisiegel U, Weber W, Ihrke G, *et al.*** The LDL-receptor-related protein, LRP, is an apolipoprotein E-binding protein. *Nature*. 1989; 341: 162–4.
15. **Strickland DK, Ashcom JD, Williams S, *et al.*** Sequence identity between the alpha 2-macroglobulin receptor and low density lipoprotein receptor-related protein suggests that this molecule is a multifunctional receptor. *J Biol Chem*. 1990; 265: 17401–4.
16. **Regina A, Demeule M, Che C, *et al.*** Antitumour activity of ANG1005, a conjugate between paclitaxel and the new brain delivery vector Angiopep-2. *Br J Pharmacol*. 2008; 155: 185–97.
17. **Abulrob A, Brunette E, Slinn J, *et al.*** *In vivo* time domain optical imaging of renal ischemia-reperfusion injury: discrimination based on fluorescence lifetime. *Mol Imaging*. 2007; 6: 304–14.
18. **Abulrob A, Brunette E, Slinn J, *et al.*** Dynamic analysis of the blood-brain barrier disruption in experimental stroke using time domain *in vivo* fluorescence imaging. *Mol Imaging*. 2008; 7: 248–62.
19. **Cisternino S, Rousselle C, Dagenais C, *et al.*** Screening of multidrug-resistance sensitive drugs by *in situ* brain perfusion in P-glycoprotein-deficient mice. *Pharm Res*. 2001; 18: 183–90.
20. **Dagenais C, Rousselle C, Pollack GM, *et al.*** Development of an *in situ* mouse brain perfusion model and its application to mdr1a P-glycoprotein-deficient mice. *J Cereb Blood Flow Metab*. 2000; 20: 381–6.
21. **Pickering M, Pickering BW, Murphy KJ, *et al.*** Discrimination of cell types in mixed cortical culture using calcium imaging: a comparison to immunocytochemical labeling. *J Neurosci Methods*. 2008; 173: 27–33.
22. **Moestrup SK, Schousboe I, Jacobsen C, *et al.*** beta2-glycoprotein-I (apolipoprotein H) and beta2-glycoprotein-I-phospholipid complex harbor a recognition site for the endocytic receptor megalin. *J Clin Invest*. 1998; 102: 902–9.
23. **Regina A, Demeule M, Che C, *et al.*** Antitumour activity of ANG1005, a conjugate between paclitaxel and the new brain delivery vector Angiopep-2. *Br J Pharmacol*. 2008; 155: 185–97.
24. **Banks WA, Goulet M, Rusche JR, *et al.*** Differential transport of a secretin analog across the blood-brain and blood-cerebrospinal fluid barriers of the mouse. *J Pharmacol Exp Ther*. 2002; 302: 1062–9.
25. **Duvernoy H, Delon S, Vannson JL.** The vascularization of the human cerebellar cortex. *Brain Res Bull*. 1983; 11: 419–80.
26. **Ito S, Ohtsuki S, Terasaki T.** Functional characterization of the brain-to-blood efflux clearance of human amyloid-beta peptide (1-40) across the rat blood-brain barrier. *Neurosci Res*. 2006; 56: 246–52.
27. **Shibata M, Yamada S, Kumar SR, *et al.*** Clearance of Alzheimer's amyloid-ss(1-40) peptide from brain by LDL receptor-related protein-1 at the blood-brain barrier. *J Clin Invest*. 2000; 106: 1489–99.
28. **Bu G, Maksymovitch EA, Nerbonne JM, *et al.*** Expression and function of the low density lipoprotein receptor-related protein (LRP) in mammalian central neurons. *J Biol Chem*. 1994; 269: 18521–8.
29. **Polavarapu R, Gongora MC, Yi H, *et al.*** Tissue-type plasminogen activator-mediated shedding of astrocytic low-density lipoprotein receptor-related protein increases the permeability of the neurovascular unit. *Blood*. 2007; 109: 3270–8.
30. **Rebeck GW, Reiter JS, Strickland DK, *et al.*** Apolipoprotein E in sporadic Alzheimer's disease: allelic variation and receptor interactions. *Neuron*. 1993; 11: 575–80.
31. **Tooyama I, Kawamata T, Akiyama H, *et al.*** Subcellular localization of the low density lipoprotein receptor-related protein (alpha 2-macroglobulin receptor) in human brain. *Brain Res*. 1995; 691: 235–8.
32. **Wolf BB, Lopes MB, VandenBerg SR, *et al.*** Characterization and immunohistochemical localization of alpha 2-macroglobulin receptor (low-density lipoprotein receptor-related protein) in human brain. *Am J Pathol*. 1992; 141: 37–42.
33. **Furian AF, Oliveira MS, Royes LF, *et al.*** GM1 ganglioside induces vasodilation and increases catalase content in the brain. *Free Radic Biol Med*. 2007; 43: 924–32.
34. **Tsuji A.** Small molecular drug transfer across the blood-brain barrier *via* carrier-mediated transport systems. *NeuroRx*. 2005; 2: 54–62.
35. **Sagare A, Deane R, Bell RD, *et al.*** Clearance of amyloid-beta by circulating lipoprotein receptors. *Nat Med*. 2007; 13: 1029–31.
36. **Williams SE, Ashcom JD, Argraves WS, *et al.*** A novel mechanism for controlling the activity of alpha 2-macroglobulin receptor/low density lipoprotein receptor-related protein. Multiple regulatory sites for 39-kDa receptor-associated protein. *J Biol Chem*. 1992; 267: 9035–40.
37. **Anderson CM, Howard A, Walters JR, *et al.*** Taurine uptake across the human intestinal brush-border membrane is *via* two transporters: H(+)-coupled PAT1 (SLC36A1) and Na(+)- and Cl(−)-dependent TauT (SLC6A6). *J Physiol*. 2009; 587: 731–44.
38. **Drain J, Bishop JR, Hajduk SL.** Haptoglobin-related protein mediates trypanosome lytic factor binding to trypanosomes. *J Biol Chem*. 2001; 276: 30254–60.
39. **Yamada K, Hashimoto T, Yabuki C, *et al.*** The low density lipoprotein receptor-related protein 1 mediates uptake of amyloid {beta} peptides in an *in vitro* model of the blood-brain barrier cells. *J Biol Chem*. 2008; 283: 34554–62.
40. **Demeule M, Currie JC, Bertrand Y, *et al.*** Involvement of the low-density lipoprotein receptor-related protein in the transcytosis of the brain delivery vector angiopep-2. *J Neurochem*. 2008; 106: 1534–44.
41. **Dolmer K, Gettins PG.** Three complement-like repeats compose the complete alpha2-macroglobulin binding site in the second ligand binding cluster of the low density lipoprotein receptor-related protein. *J Biol Chem*. 2006; 281: 34189–96.
42. **Wu SM, Boyer CM, Pizzo SV.** The binding of receptor-recognized alpha2-macroglobulin to the low density lipoprotein receptor-related protein and the alpha2M signaling receptor is decoupled by oxidation. *J Biol Chem*. 1997; 272: 20627–35.
43. **Liu Z, Winters M, Holodniy M, *et al.*** siRNA delivery into human T cells and primary cells with carbon-nanotube transporters. *Angew Chem Int Ed Engl*. 2007; 46: 2023–7.

44. **Warshawsky I, Herz J, Broze GJ Jr, *et al.*** The low density lipoprotein receptor-related protein can function independently from heparan sulfate proteoglycans in tissue factor pathway inhibitor endocytosis. *J Biol Chem*. 1996; 271: 25873–9.
45. **Vives E.** Cellular uptake [correction of utake] of the Tat peptide: an endocytosis mechanism following ionic interactions. *J Mol Recognit*. 2003; 16: 265–71.
46. **Rusnati M, Urbinati C, Caputo A, *et al.*** Pentosan polysulfate as an inhibitor of extracellular HIV-1 Tat. *J Biol Chem*. 2001; 276: 22420–5.
47. **Gosselet F, Candela P, Sevin E, *et al.*** Transcriptional profiles of receptors and transporters involved in brain cholesterol homeostasis at the blood-brain barrier: use of an *in vitro* model. *Brain Res*. 2009; 1249: 34–42.
48. **Tirona RG, Kim RB.** Pharmacogenomics of organic anion-transporting polypeptides (OATP). *Adv Drug Deliv Rev*. 2002; 54: 1343–52.
49. **Deane R, Du Yan S, Submamaryan RK, *et al.*** RAGE mediates amyloid-beta peptide transport across the blood-brain barrier and accumulation in brain. *Nat Med*. 2003; 9: 907–13.
50. **Herve F, Ghinea N, Scherrmann JM.** CNS delivery *via* adsorptive transcytosis. *AAPS J*. 2008; 10: 455–72.
51. **Wender PA, Mitchell DJ, Pattabiraman K, *et al.*** The design, synthesis, and evaluation of molecules that enable or enhance cellular uptake: peptoid molecular transporters. *Proc Natl Acad Sci USA*. 2000; 97: 13003–8.
52. **Suzuki T, Futaki S, Niwa M, *et al.*** Possible existence of common internalization mechanisms among arginine-rich peptides. *J Biol Chem*. 2002; 277: 2437–43.
53. **Gaillard PJ, Visser CC, de Boer AG.** Targeted delivery across the blood-brain barrier. *Expert Opin Drug Deliv*. 2005; 2: 299–309.
54. **Pardridge WM.** The blood-brain barrier: bottleneck in brain drug development. *NeuroRx*. 2005; 2: 3–14.
55. **Ghose AK, Viswanadhan VN, Wendoloski JJ.** A knowledge-based approach in designing combinatorial or medicinal chemistry libraries for drug discovery. 1. A qualitative and quantitative characterization of known drug databases. *J Comb Chem*. 1999; 1: 55–68.
56. **Lipinski CA.** Drug-like properties and the causes of poor solubility and poor permeability. *J Pharmacol Toxicol Methods*. 2000; 44: 235–49.